AN AUSM-BASED THIRD-ORDER COMPACT SCHEME FOR SOLVING EULER EQUATIONS

M. A. H. Mohamad[1], S. Basri[1], I. Abd. Rahim[2] and M. Mohamad[3]
[1]Dept. of Aerospace Engineering, Faculty of Engineering, Universiti Putra Malaysia, Selangor, Malaysia.
[2]Dept. of Plant & Automotive Engineering, Faculty of Mechanical & Manufacturing Engineering,
University College of Technology Tun Hussein Onn, Johor, Malaysia.
[3]Dept. of Mathematics, Science Studies Centre, University College of Technology Tun Hussein Onn,
Johor, Malaysia.
E-mail: hakim@kuittho.edu.my

ABSTRACT

In this paper, a third-order compact upwind scheme is given for calculating flows containing discontinuities. The scheme utilizes the AUSM flux splitting method and a third-order compact upwind space discretization relation for calculating third-order numerical flux function. TVD shock capturing properties of the scheme are achieved through a minmod flux limiter. A multistage TVD Runge-Kutta method is employed for the time integration. Computations are performed for two typical one-dimensional problems containing shocks, namely, the steady flow in a divergent nozzle and the unsteady shock tube problem. First-order and third-order numerical results are presented in comparison with the exact solutions. Computed results with KFVS method are also presented.

Key words*: Third-Order Compact Upwind Scheme, AUSM scheme, KFVS scheme*

INTRODUCTION

High-order compact schemes have attracted much attention in recent years due to their narrow grid stencil and a possible enhanced accuracy over the non-compact schemes [1]. Different approaches for high-order compact spatial discretization have been proposed during the last 25 years.

Lele [1] has presented and analyzed a class of high-order central schemes and introduced the notion of resolution efficiency. Central compact schemes have been used for solving inviscid flows [2] and viscous flows [3,4,5]. However, numerical instabilities and spurious oscillations are often encountered in the solution of convection-dominated flows. These instabilities can be suppressed either by adding high-order dissipation terms [2] or by using filtering [4].

Shock discontinuities give rise to high frequency oscillations even in smooth regions of the flow due to odd-even decoupling. Therefore, excessive smoothing is required to capture strong shocks. This in turn will considerably degrade the solution scheme. Consequently, central schemes are not robust enough for flows with discontinuities. On the other hand, upwind schemes are expected to be more robust and to yield superior results. Cockburn and Shu [6], using the idea of TVD (total variation diminishing) with a modified flux limiter, have formulated a family of nonlinear stable compact schemes for nonlinear scalar conservation laws. Upwinding is introduced through Lax-Friedrichs flux-splitting method.

Deng and Maekawa [7] have presented higher-order nonlinear schemes for capturing discontinuities. They used Roe's approximate Riemann solver and a fourth-order cell-centered compact scheme to calculate higher-order numerical flux at a cell interface. The left and right states are computed through compact adaptive interpolation in the spirit of ENO [8] reconstruction. The drawback of Roe's approximate Riemann solver and ENO schemes is that they are computationally uneconomical. Ravichandran [9] has developed a third-order flux-splitting variant TVD upwind scheme. Only steady state results are reported.

In general, upwind schemes are categorized as either FDS (flux difference splitting) or FVS (flux vector splitting). The most popular FDS scheme is the Roe's [10] scheme due to its accuracy and efficiency. The FVS schemes, such as Steger and Warming's [11], van Leer's [12] and KFVS [13] are known to be simple and robust

for capturing of intense shocks and rarefaction waves. However, while FVS is based on scalar calculations and FDS is based on matrix calculations.

The high-order compact schemes developed by Cockburn and Shu [6], Mawlood *et al.* [14], and Ravichandran [9] among others are examples of FVS schemes. The drawback of FVS methods is that they have accuracy problems in resolving shear layer regions due to the excessive numerical dissipation error associated with them.

Liou and Steffen [15] have proposed AUSM (Advection Upstream Splitting Method) that has the accuracy of FDS schemes and the robustness and efficiency of FVS schemes. In this method, the inviscid flux at a cell interface is split into a convective contribution, upwinded in the direction of the flow and a pressure contribution which is upwinded based on acoustic considerations. The direction of the flow is determined by the sign of a Mach number defined by combining information from both the left and right states about the cell interface.

The main purpose of the present work is to develop a high-order compact shock capturing scheme based on AUSM flux splitting method. A third-order, upwind-based compact scheme proposed by Zhong [16] is used to obtain the higher-order numerical fluxes. TVD shock capturing properties are obtained through the minmod flux limiters presented by Cockburn and Shu [6] and Ravichandran [9]. The scheme is tested with two typical one dimensional problems containing shocks. The first problem is a steady supersonic-subsonic flow in a divergent nozzle and the second is a time dependent shock tube problem. First-order and third-order results are presented in comparison with the exact solutions. Results using the KFVS method [13] are also presented.

THE BASIC DISCRETIZATION METHOD

Spatial Discretization and Numerical Fluxes

The model equation for nonlinear scalar conservation law in one-dimensional space can be written as [10,11]

$$\frac{\partial u}{\partial t} + \frac{\partial f(u)}{\partial x} = 0 \tag{1}$$

with the subject to the given initial condition [10,11]

$$u(x,0) = u_0(x) \tag{2}$$

where $\dfrac{\partial f(u)}{\partial x}$ is some vector-valued function of u. Equation (2), is specialised to

$$u(x,0) \equiv u_L (x < 0)$$
$$u(x,0) \equiv u_R (x > 0) \tag{3}$$

Equation (1) can be written in split flux form as [9]

$$\frac{\partial u}{\partial t} + \frac{\partial f^+(u)}{\partial x} + \frac{\partial f^-(u)}{\partial x} = 0 \tag{4}$$

where $f(u) = f^+(u) + f^-(u)$. This flux vector splitting has been introduced by [11]. The split fluxes $f^+(u)$ and $f^-(u)$ are also homogeneous functions of degree one in u [18]. Conservative semidiscretization of equation (4) can be written as [9]

$$\frac{\partial u_i}{\partial t} + (\hat{f}_{i+1/2} - \hat{f}_{i-1/2}) / \Delta x = 0 \tag{5}$$

where $\hat{f}_{i+1/2}$ and $\hat{f}_{i-1/2}$ is known as the numerical flux function.

First-order upwind approximation to the numerical flux is given by [9]

$$\hat{f}_{i+1/2} = f_i^+ + f_{i+1}^-$$
$$\hat{f}_{i-1/2} = f_{i-1}^+ - f_i^-$$
(6)

Following Ravichandran [9], a high-order numerical flux can be obtained as follows. The numerical flux $\hat{f}_{i+1/2}$ is decomposed into positive and negative parts, $\hat{f}_{i+1/2}^+$ and $\hat{f}_{i+1/2}^-$ such that

$$\hat{f}_{i+1/2} = \hat{f}_{i+1/2}^+ + \hat{f}_{i+1/2}^-$$
(7)

The decomposed numerical fluxes are defined such that

$$F_i^{\mp} = \hat{f}_{i+1/2}^{\mp} - \hat{f}_{i-1/2}^{\mp}$$
(8)

where $F_i^{\mp} / \Delta x$ is a high-order approximation to the derivative $\dfrac{\partial f^{\mp}(u_i)}{\partial x}$, to be determined by a high-order compact scheme.

Zhong [16] has presented a third-order approximation to a first derivative by an upwind based compact relation as

$$18.75 F_{i\pm1}^{\mp} + 60 F_i^{\mp} + 15 F_{i\mp1}^{\mp} = \pm 52.5 f_{i\pm1}^{\mp} \mp 15 f_i^{\mp} \mp 37.5 f_{i\mp1}^{\mp}$$
(9)

Equation (9) can be written for the interior points $i = 2$ to $i = N - 1$. For the boundary points $i = 1$ and $i = N$, the following second order explicit relations are used

$$F_1^{\mp} = -1.5 f_1^{\mp} + 2 f_2^{\mp} - 0.5 f_3^{\mp}$$
(10)
$$F_N^{\mp} = 1.5 f_N^{\mp} - 2 f_{N-1}^{\mp} + 0.5 f_{N-2}^{\mp}$$
(11)

Plugging equation (8) in equation (9) yields the following relations for the interior points $i = 2$ to $i = N - 1$.

$$18.75 \hat{f}_{i-1/2}^+ + 60 \hat{f}_{i+1/2}^+ + 11.25 \hat{f}_{i+3/2}^+ = 37.5 f_{i+1}^+ + 52.5 f_i^+$$
(12)
$$11.25 \hat{f}_{i-1/2}^- + 60 \hat{f}_{i+1/2}^- + 18.75 \hat{f}_{i+3/2}^- = 52.5 f_{i+1}^- + 37.5 f_i^-$$
(13)

With $F_1^{\mp}$ and $F_N^{\mp}$ evaluated explicitly, two sets of (N - 1) equations are to be inverted for the split numerical fluxes $\hat{f}_{i+1/2}^{\mp}$. Before using these fluxes it is necessary to limit their values and this is achieved by defining the differences

$$d\hat{f}_{i+1/2}^+ = \hat{f}_{i+1/2}^+ - f_i^+$$
$$d\hat{f}_{i+1/2}^- = f_{i+1}^- - \hat{f}_{i+1/2}^-$$
(14)

and limiting by the limiter

$$df\hat{}_{i+1/2}^{+(m)} = \min \text{mod}(d\hat{f}_{i+1/2}^{+}, D^{+})$$
$$df\hat{}_{i+1/2}^{-(m)} = \min \text{mod}(d\hat{f}_{i+1/2}^{-}, D^{-})$$

(15)

The third-order TVD flux differences of [17] may be used here

$$D^{+} = \frac{1}{6}(\text{minmod}(\delta^{+}f_{i-1}^{+}, \lambda\delta^{+}f_{i}^{+}) + 2\min\text{mod}(\delta^{+}f_{i}^{+}, \lambda\delta^{+}f_{i-1}^{+}))$$

(16)

$$D^{-} = \frac{1}{6}(\min\text{mod}(\delta^{+}f_{i+1}^{-}, \lambda\delta^{+}f_{i}^{-}) + 2\min\text{mod}(\delta^{+}f_{i}^{-}, \lambda\delta^{+}f_{i+1}^{-}))$$

(17)

where $1 \leq \lambda \leq 4$.

The limited numerical fluxes are then calculated from

$$\hat{f}_{i+1/2}^{+(m)} = f_{i}^{+} + d\hat{f}_{i+1/2}^{+(m)}$$
$$\hat{f}_{i+1/2}^{-(m)} = f_{i+1}^{-} - d\hat{f}_{i+1/2}^{-(m)}$$

(18)

and

$$\hat{f}_{i+1/2}^{(m)} = \hat{f}_{i+1/2}^{+(m)} + \hat{f}_{i+1/2}^{-(m)}$$

(19)

The min mod function can be defined as

$$\min \text{mod}(a,b) = \begin{cases} a & if \ |a| < |b|, \ (ab) > 0 \\ b & if \ |b| < |a|, \ (ab) > 0 \\ 0 & if \ (ab) < 0 \end{cases}$$

(20)

EULER EQUATIONS AND FLUX SPLITTING SCHEME

The one-dimensional Euler equation may be written as

$$\frac{\partial Q}{\partial t} + \frac{\partial E}{\partial x} = 0$$

(21)

where

$$Q = \begin{bmatrix} \rho \\ \rho u \\ \rho e \end{bmatrix}, \ E = \begin{bmatrix} \rho u \\ \rho u^{2} + p \\ \rho u H \end{bmatrix}$$

and ρ, u, p, e and H are the density, velocity, pressure, total energy, and total enthalpy respectively. The total enthalpy H, is related to the other quantities by the relation

$$H = e + \frac{p}{\rho} \qquad (22)$$

and for a perfect gas

$$e = \frac{p}{\rho(\gamma - 1)} + \frac{1}{2}u^2 \qquad (23)$$

where γ is the ratio of specific heat and takes the value of 1.4 for air.

The extension of the scalar high order numerical fluxes developed above to Euler equations is straightforward. The AUSM flux splitting technique used here is detailed in references [15,16]. Once the split fluxes $E_i^{\pm}$ are obtained then the method described above is used to obtain the higher order numerical fluxes. Equation (18) is, thus, written in a semidiscretized form as

$$\frac{\partial Q}{\partial t} = L(Q) \qquad (24)$$

where

$$L(Q) = -(\hat{E}_{i+1/2}^{(m)} - \hat{E}_{i-1/2}^{(m)})/\Delta x \qquad (25)$$

Using the method-of-lines [9], the systems of equations (21) are integrated by a multistage TVD Runge-Kutta scheme [17].

BOUNDARY CONDITIONS

For the supersonic-subsonic nozzle problem considered in this paper, one type of boundary conditions i.e. inflow/outflow is encountered. At the supersonic inflow, values of velocity, density and pressure are specified while at the subsonic outflow the velocity is specified and the density and pressure are extrapolated from the interior. For the shock tube problem, a short time span for unsteady flow is considered such that the waves will not reach the end walls and so conditions at these boundaries are held fixed.

RESULTS AND DISCUSSIONS

In this study, two problems are considered as test cases for the developed scheme. Results are presented for both the AUSM and the KFVS variants of the scheme. Results are also shown with first-order accurate upwind space discretization. The first problem considered is a quasi one-dimensional supersonic-subsonic flow in a divergent nozzle. The nozzle cross-section $S(x)$ varies according to

$$S(x) = 1.398 + 0.347 \tanh\big(0.8(x - 4)\big); \qquad 0 \le x \le 10$$

The inflow and outflow conditions are

$$
\begin{aligned}
(\rho_1, u_1, p_1) \qquad &= (0.459, 432.5, 0.2724 \times 10^5) \\
(\rho_N, u_N, p_N) \qquad &= (0.811, 146.94, 0.673 \times 10^5)
\end{aligned}
$$

These conditions correspond to a normal shock at $x = 5$ with supersonic flow at the inlet Mach number $M_1 = 1.5$ and subsonic flow at the outlet Mach number $M_N = 0.431$. Calculation are performed with a time step, Δt corresponding to Courant-Friedrichs-Lewy, CFL number = 1. The number of points used to solve this problem is N = 51. The integration in time is continued until steady state is reached. The solution is assumed to converge when the absolute value of the residual in pressure $\left| p^{n+1} - p^n \right| \le 0.1$.

Fig. 1 shows first-order upwind results for the distribution of pressure, density and Mach number along the flow in comparison with the exact solution. The solution are oscillation free, however, shock smearing, due to high

false diffusion of first-order upwinding, is evident with both flux splitting methods. In Fig. 2 results obtained by the third-order schemes are shown. The shock capturing properties of the AUSM are improved while the KFVS method produces oscillatory solution behind the shock.

The second problem considered is the unsteady shock tube problem. This problem is an interesting test case to assess the ability of a compressible code to capture shocks and contact discontinuities and to produce exact profiles in the rarefaction wave. The problem spatial domain is $0 \leq x \leq 1$. The initial solution of the problem consists of two uniform states, termed as left and right states, separated by a discontinuity at $x = 0.5$. As in the first problem, results are obtained using first-order and third-order upwind schemes with both the AUSM and the KFVS methods. The number of mesh points used is 101 and CFL = 0.2. The initial conditions of the left and right states are

$$(\rho_L, u_L, p_L) = (1, 0, 1)$$
$$(\rho_R, u_R, p_R) = (0.125, 0, 0.1)$$

The wave pattern of this problem consists of a rightward moving shock wave, a leftward moving rarefaction wave and a contact discontinuity separating the shock and rarefaction waves and moving rightward. Fig. 3 shows results obtained by the first order accurate schemes for the distribution of pressure, density and velocity along the tube at time, $t = 0.2$ units, in comparison with the exact solution. Although the solution contains no oscillations the smearing of all types of discontinuities is quite clear. In Fig. 4 the third-order results are shown. The improvement in resolving the different types of discontinuities is clear. The shock discontinuity is resolved more accurately by the AUSM scheme as can be seen from the velocity plot. The contact discontinuity is resolved equally by both schemes; however, a small jump is observed ahead of the contact discontinuity in the result of the AUSM scheme as can be seen in the density and velocity plots. The calculated profiles of all variables in the rarefaction wave agree very well with the exact solution. The KFVS variant shows slightly better accuracy than the AUSM variant.
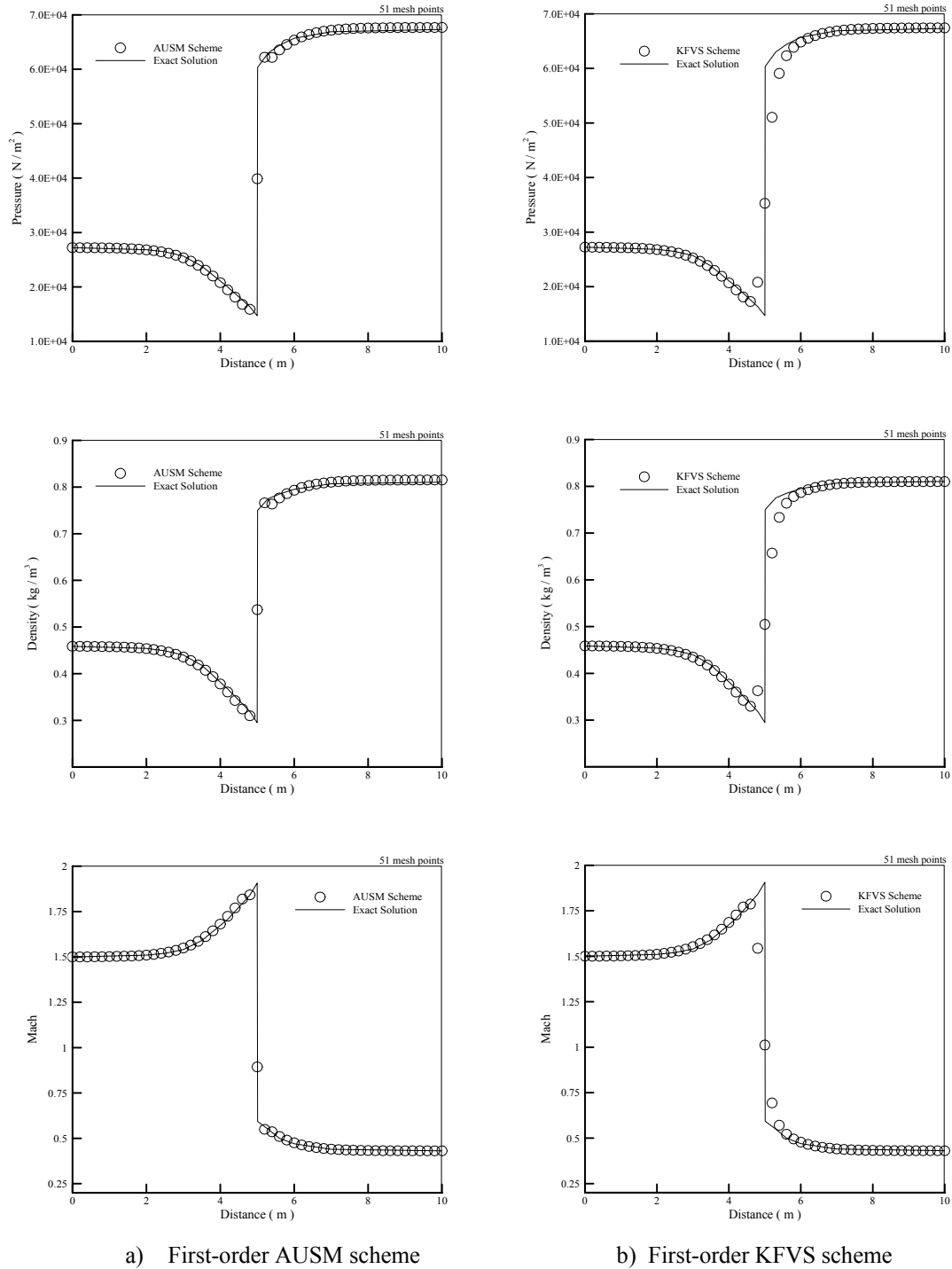
a)   First-order AUSM scheme   b) First-order KFVS scheme

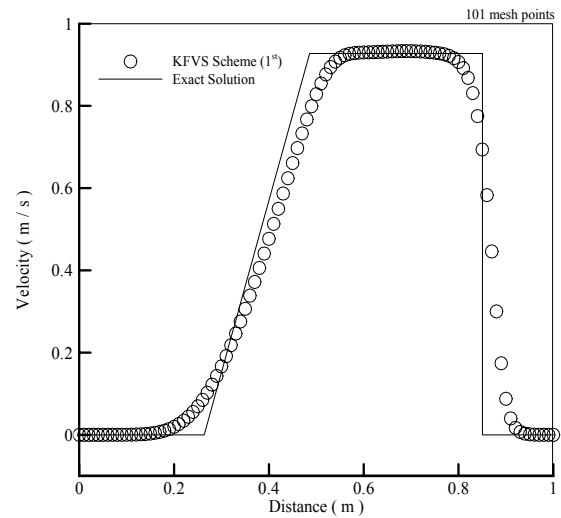*Figure 1: Results for steady supersonic-subsonic flow in a diverging nozzle, 51 mesh points at CFL = 1.0.*
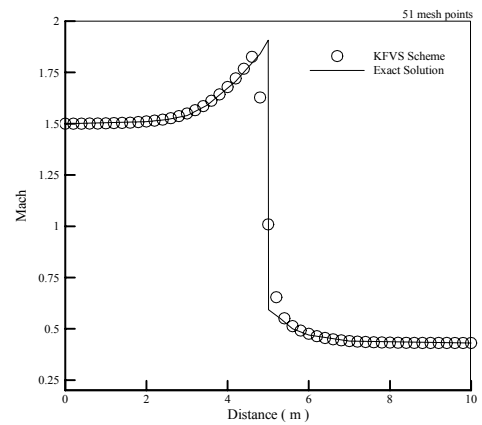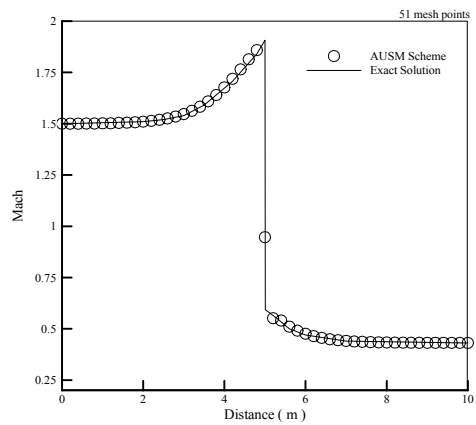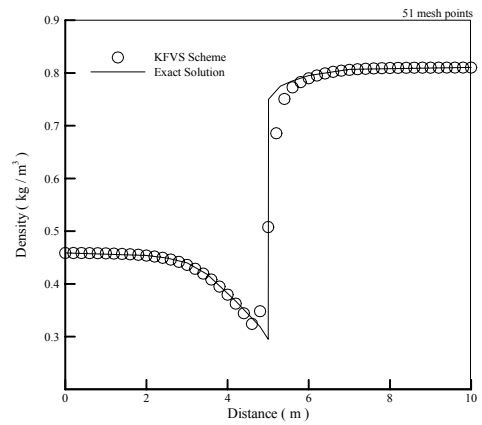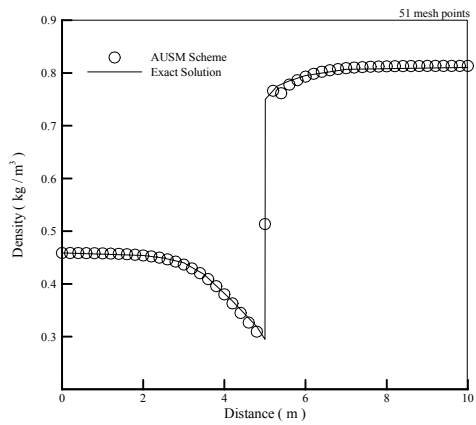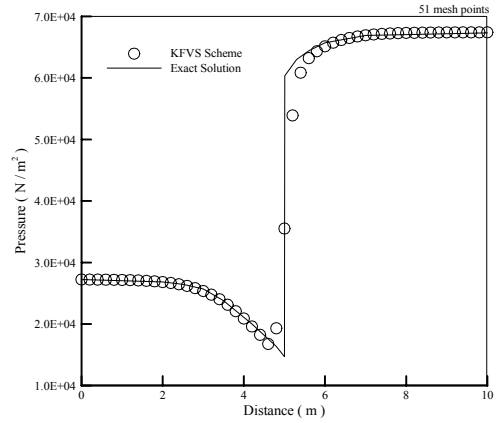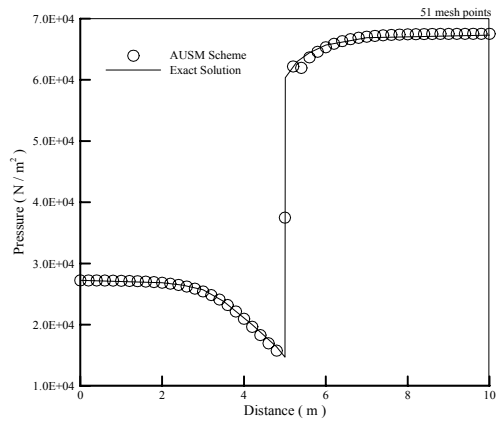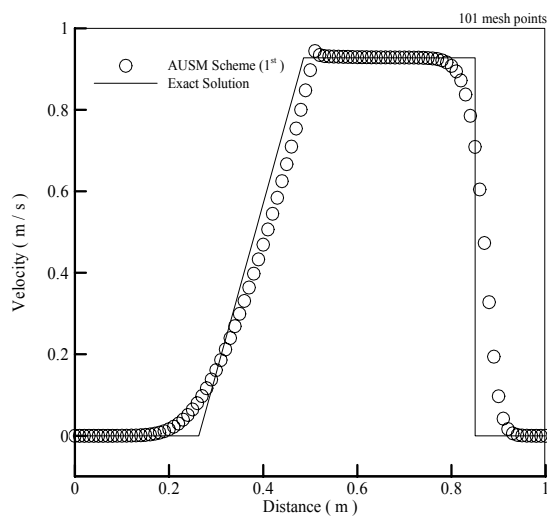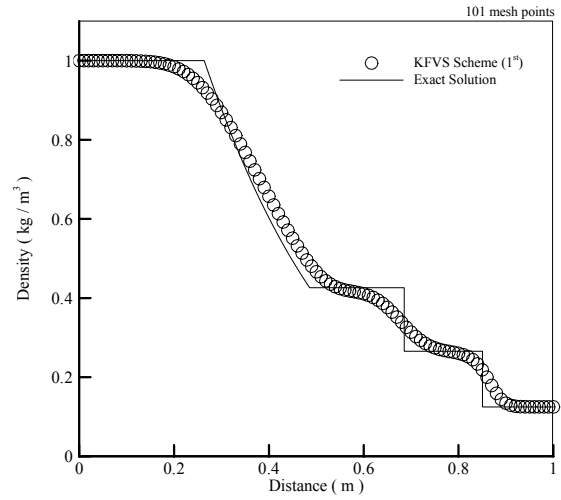
a) Third-order AUSM scheme   b) Third-order KFVS scheme

Figure 2: Results for steady supersonic-subsonic flow in a diverging nozzle, 51 mesh points at CFL = 1.0.
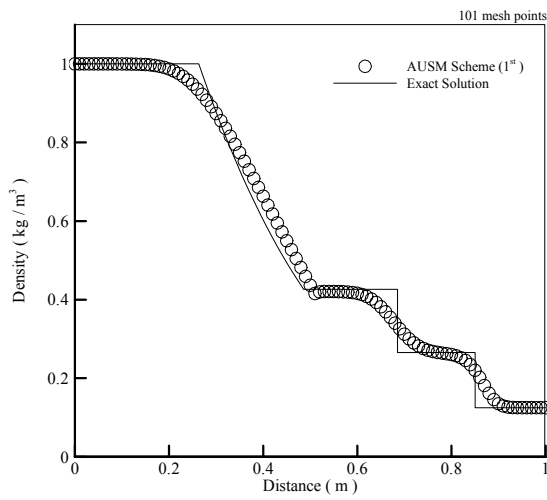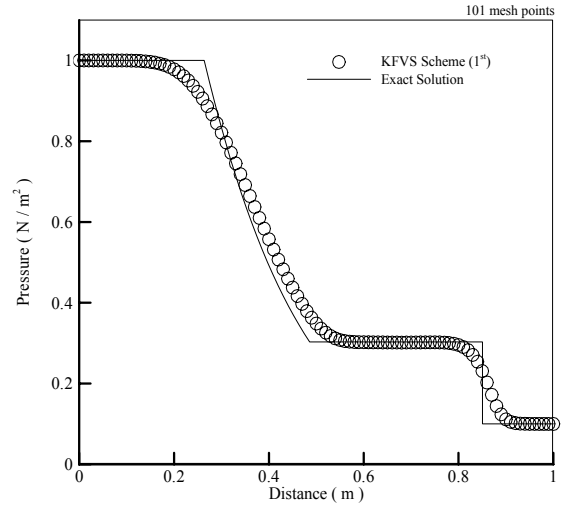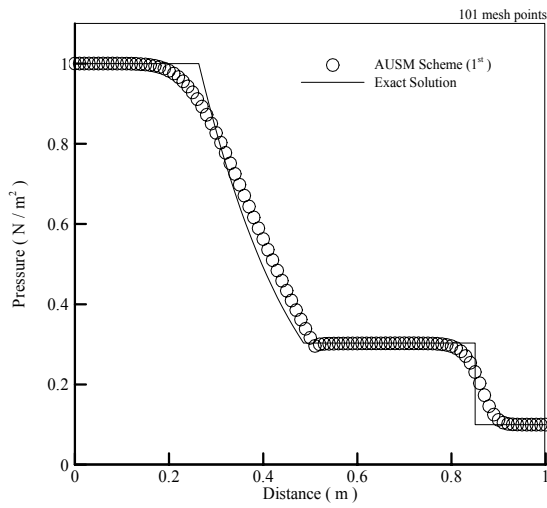
a) First-order AUSM scheme   b) First-order KFVS scheme

Figure 3: First-order results for the shock tube problem, 101 mesh points at CFL = 0.2.

a) Third-order AUSM scheme
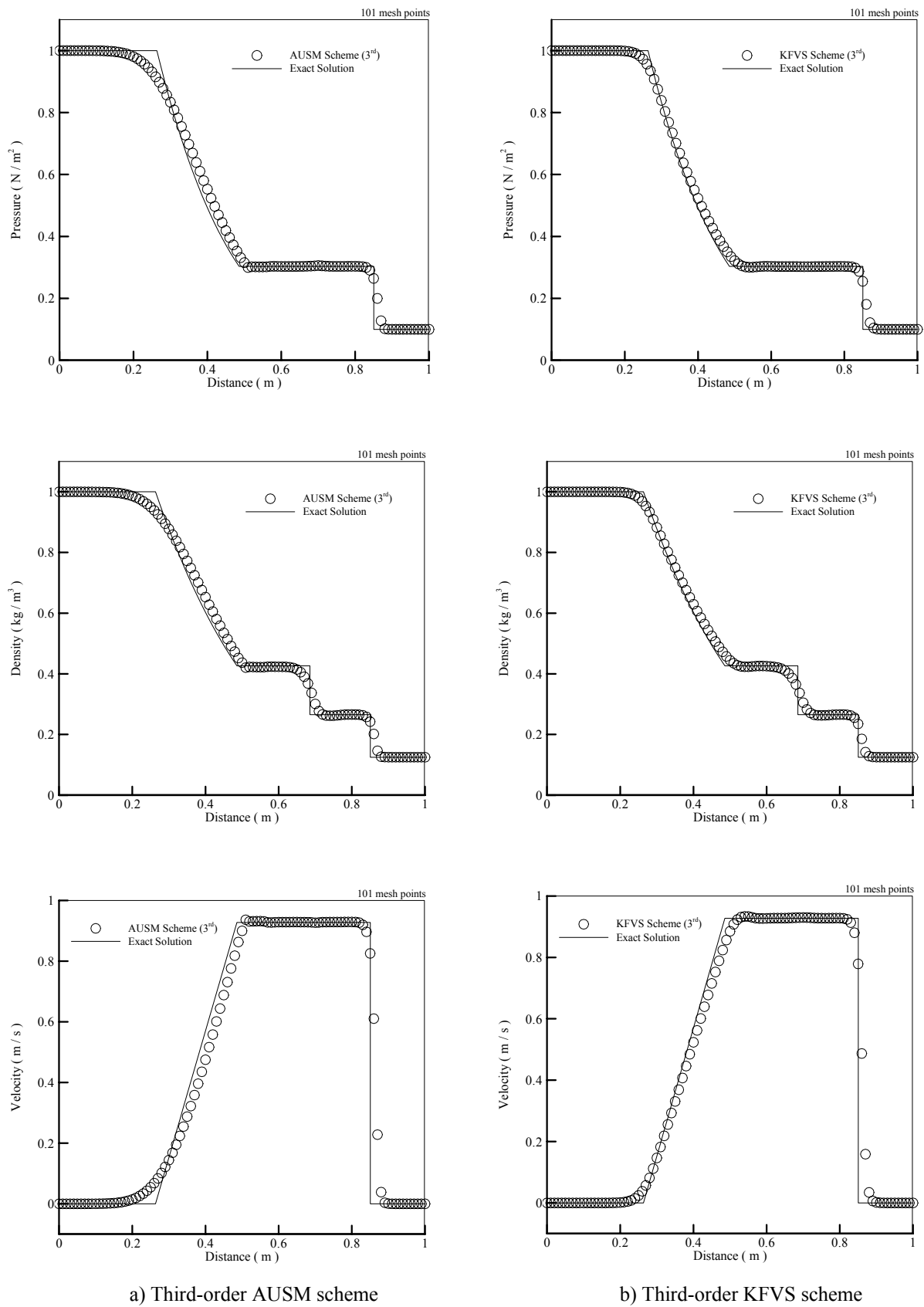
b) Third-order KFVS scheme

Figure. 4: Third-order results for the shock tube problem, 101 mesh points at CFL = 0.2.

CONCLUSIONS

A third-order accurate TVD compact shock-capturing scheme is developed using the AUSM flux splitting method. The scheme is tested by performing calculations for a quasi one-dimensional supersonic-subsonic nozzle flow and a shock tube problem. Results are also presented with a scheme based on KFVS. The KFVS variant has shown oscillations behind the stationary shock wave in the nozzle flow problem. However, the KFVS variant is found to capture contact and rarefaction discontinuities in the shock tube problem more accurately than the AUSM variant.

REFERENCES

[1]   Lele, S. K. (1992) Compact Finite Difference Schemes with Spectral-Like Resolution. Journal of Computational Physics, **103**:16-42.

[2]   Ekaterinaris, J. A. (1999) Implicit High–Resolution, Compact Schemes for Gas Dynamics and Aeroacoustics. Journal of Computational Physics, **156**: 272-299.

[3]   Ekaterinaris, J. A. (2000) Implicit High-Order Accurate In-Space Algorithms for The Navier Stokes Equations. AIAA Journal, **38**:1591-1602.

[4]   Visbal, M. R. and Gaitonde, P. V. (1999) High Order-Accurate Methods for Complex Unsteady Subsonic Flows. AIAA Journal, **10**: 358-366.

[5]   Mawlood, M. K., Asrar, W., Basri, S. and Ahmad, M. H. M. (2001) High-Order Compact Finite Difference Solution of Navier-Stoke Equations. Jurnal Mekanikal, **12**: 83-95.

[6]   Cockburn, B. and Shu, C. W. (1994) Nonlinearly Stable Compact Schemes for Shock Calculation. SIAM Journal on Numerical Analysis, **31**(3): 607-627.

[7]   Deng, X. and Maekawa, H. (1997) Compact High–Order Accurate Nonlinear Schemes. Journal of Computational Physics, **130**: 77-91.

[8]   Harten, A., Engquist, B., Osher, S. and Chakravarthy, S. (1987) Uniformly High Order Accurate Essentially Non-Oscillatory Schemes, III. Journal of Computational Physics, **71**: 231-303.

[9]   Ravichandran, K. S. (1997) High Order KFVS Algorithms Using Compact Upwind Difference Operators. Journal of Computational Physics, **130**: 161-173.

[10]   Roe, P. L. (1981) Approximate Riemann Solvers, Parameter Vectors, and Difference Schemes. Journal of Computational Physics, **43**: 357-372.

[11]   Steger, J. L. and Warming, R. F. (1981) Flux Vector Splitting of the Inviscid Gas Dynamic Equations with Application to Finite Difference Methods. Journal of Computational Physics, **40**: 263-293.

[12]   Van Leer, B. (1982) Flux Vector Splitting for the Euler Equation. Lecture Notes in Physics, **170**: 507-512.

[13]   Deshpande, S. M. and Kulkarni, P. S. (1998) New Developments in Kinetic Schemes. Computers Math. Application, **35**(112): 75-93.

[14]   Mawlood, M. K., Asrar, W., Omar, A.A. and Basri, S. (2003) A High-Resolution Compact Upwind Algorithm for Inviscid Flows. 41st Aerospace Sciences Meeting and Exhibit Conference, AIAA 2003-0076, USA.

[15]   Liou, M. S. and Steffen, C. J. Jr. (1993) A New Flux Splitting Scheme. Journal of Computational Physics, **107**: 23-39.

[16]   Zhong, X. (1998) High-Order Finite-Difference Schemes for Numerical Simulation of Hypersonic Boundary-Layer Transition. Journal of Computational Physics, **144**: 662-709.

[17]   Yee, H. C. (1987) Upwind and Symmetric Shock Capturing Schemes. NASA TM 89464.

[18]   Hirsch, C. (1990) Numerical Computation of Internal and External Flows. Vol. 2: Computational Methods for Inviscid and Viscous Flows. John Wiley and Sons, UK.

ABBREVIATIONS

AUSM	Advection upstream splitting method
CFL	Courant-Friedrichs-Lewy number
ENO	Essentially non-oscillatory schemes
FDS	Flux-difference splitting
FVS	Flux-vector splitting
KFVS	Kinetic flux-vector splitting
TVD	Total variation diminishing

NOTATIONS

a, b	Coefficients in high-order compact schemes
$\hat{df}$	Flux difference
D	Diffusion number
E	Flux vectors
e	Total energy
F_i	High-order approximation to first derivative
F	Flux vectors
f	Scalar flux
$\hat{f}$	Flux function
H	Total enthalpy
i	Inner layer
L	Characteristic length
M	Mach number
N	Maximum number of grid points
p	Pressure
Q	Conservative variable vector
u	Velocity components
λ	Eigenvalue
δ^+	Forward difference operators
Δ	Increment in time and space
γ	Specific heat ratio, for air = 1.4
ρ	Density

Superscripts
n	n-th time level
m	Modified (limited) flux

Subscripts
l, N	Inflow and outflow condition
L, R	Left and right states
0	Outer layer